

## A distributed charge storage with GeO<sub>2</sub> nanodots

T. C. Chang, S. T. Yan, C. H. Hsu, M. T. Tang, J. F. Lee, Y. H. Tai, P. T. Liu, and S. M. Sze

Citation: *Applied Physics Letters* **84**, 2581 (2004); doi: 10.1063/1.1697627

View online: <http://dx.doi.org/10.1063/1.1697627>

View Table of Contents: <http://scitation.aip.org/content/aip/journal/apl/84/14?ver=pdfcov>

Published by the [AIP Publishing](#)

---

### Articles you may be interested in

First-principles study on the effective masses of zinc-blend-derived Cu<sub>2</sub>Zn<sub>1-4x</sub>IVVI<sub>4</sub> (IV=Sn, Ge, Si and VI=S, Se)

*J. Appl. Phys.* **112**, 093717 (2012); 10.1063/1.4759322

Structure and physical properties of Ge<sub>x</sub>As<sub>y</sub>Se<sub>1-x-y</sub> glasses with the same mean coordination number of 2.5

*J. Appl. Phys.* **109**, 023517 (2011); 10.1063/1.3544309

Density and concentration fluctuations in SiO<sub>2</sub>-GeO<sub>2</sub> optical fiber glass investigated by small angle x-ray scattering

*J. Appl. Phys.* **103**, 094917 (2008); 10.1063/1.2917384

Orientation of pentacene molecules on SiO<sub>2</sub>: From a monolayer to the bulk

*J. Chem. Phys.* **126**, 154702 (2007); 10.1063/1.2717161

Characteristics of ZrO<sub>2</sub> gate dielectrics on O<sub>2</sub>- and N<sub>2</sub>O-plasma treated partially strain-compensated Si<sub>0.69</sub>Ge<sub>0.3</sub>C<sub>0.01</sub> layers

*J. Appl. Phys.* **100**, 034105 (2006); 10.1063/1.2227269

---

The advertisement features a dark blue background with white and orange text. At the top left, it reads 'NEW! Asylum Research MFP-3D Infinity™ AFM' in large white letters, followed by 'Unmatched Performance, Versatility and Support' in orange. To the right is the Oxford Instruments logo, which includes the text 'OXFORD INSTRUMENTS' and the tagline 'The Business of Science®'. Below the main text are four images: a blue textured surface, a brown textured surface, a grid of small square samples, and the MFP-3D Infinity AFM instrument itself. Each image is accompanied by a short text description: 'Stunning high performance', 'Simpler than ever to GetStarted™', 'Comprehensive tools for nanomechanics', and 'Widest range of accessories for materials science and bioscience'.

## A distributed charge storage with GeO<sub>2</sub> nanodots

T. C. Chang<sup>a)</sup>

*Department of Physics and Institute of Electro-Optical Engineering, National Sun Yat-Sen University, Kaohsiung, Taiwan, Republic of China and Center for Nanoscience & Nanotechnology, National Sun Yat-sen University, 70 Lien-hai Road, Gushan Chiu, Kaohsiung, Taiwan 804, Republic of China*

S. T. Yan

*Institute of Electronics, National Chiao Tung University, Hsin-Chu, Taiwan, Republic of China*

C. H. Hsu, M. T. Tang, and J. F. Lee

*National Synchrotron Radiation Research Center, Hsin-Chu, Taiwan 300, Republic of China*

Y. H. Tai

*The Institute of Electro-Optical Engineering, National Chiao Tung University, Hsin-Chu, Taiwan, Republic of China*

P. T. Liu and S. M. Sze

*National Nano Device Laboratory, 1001-1 Ta-Hsueh Road, Hsin-Chu 300, Taiwan, Republic of China*

(Received 24 November 2003; accepted 19 February 2004)

In this study, a distributed charge storage with GeO<sub>2</sub> nanodots is demonstrated. The mean size and aerial density of the nanodots embedded in SiO<sub>2</sub> are estimated to be about 5.5 nm and  $4.3 \times 10^{11} \text{ cm}^{-2}$ , respectively. The composition of the dots is also confirmed to be GeO<sub>2</sub> by x-ray absorption near-edge structure analyses. A significant memory effect is observed through the electrical measurements. Under the low voltage operation of 5 V, the memory window is estimated to  $\sim 0.45$  V. Also, a physical model is proposed to demonstrate the charge storage effect through the interfacial traps of GeO<sub>2</sub> nanodots. © 2004 American Institute of Physics.

[DOI: 10.1063/1.1697627]

Due to the high cost, large volume, and high power consumption of the magnetic-core memory, the electronic industries urgently needed a new kind of memory device to replace the magnetic-core memory in the 1960s. In 1967, Kahng and Sze invented the first floating-gate (FG) nonvolatile semiconductor memory at Bell Labs.<sup>1</sup> To date, the stacked-gate FG device structure continues to be the most prevailing nonvolatile-memory implementation, and is widely used in both standalone and embedded memories. The invention of FG memory impacts more than the replacement of magnetic-core memory, and creates an era of portable electronic systems. The most widespread memory array organization is the so-called flash memory, which has a byte-selectable write operation combined with a sector “flash” erase.

Although a huge commercial success, conventional FG devices have their limitations. The most prominent one is the limited potential for continued scaling of the device structure. This scaling limitation stems from the extreme requirement put on the tunnel oxide layer. On the one hand, the tunnel oxide has to allow quick and efficient charge transfer to and from the FG. On the other hand, the tunnel oxide needs to provide superior isolation under retention and disturbed conditions in order to maintain information integrity over periods of up to a decade. When the tunnel oxide is thinner for the first consideration, the retention characteristics may be degraded. And when the tunnel oxide is made thicker to take the isolation into account, the speed of the

operation will be slower. There is, therefore, a tradeoff between speed and reliability and the thickness of the tunnel oxide is compromised to about 8–11 nm, which is barely reduced over more than five successive generations of the industry.<sup>2</sup> To overcome the scaling limits of the conventional FG structure, two candidates are mostly mentioned, SONOS<sup>3–5</sup> and nanocrystal nonvolatile memory devices.<sup>6–8</sup> As for SONOS, the nitride layer is used as the charge-trapping insulator. The intrinsic distributed storage takes an advantage of the SONOS device over the FG device, its improved endurance, since a single defect will not cause the discharge of the memory.<sup>5</sup> Tiwari *et al.*<sup>6</sup> for the first time demonstrated the Si nanocrystal floating gate memory device in the early 1990s. Also, the nanocrystal memory device can maintain good retention characteristics when tunnel oxide is thinner and lower the power consumption.<sup>6–8</sup> In this contribution, a GeO<sub>2</sub> nano-dot memory device with 4.5-nm-thick tunnel oxide and a low operating voltage of 5 V is proposed. Insulating nano-dots are utilized as the storage elements rather than the semiconducting counterparts. The concepts of SONOS and nanocrystal memories are combined and explored. A significant memory effect due to the charge trapping in the GeO<sub>2</sub> dots is observed.

First, the 6 in. Si wafer was cleaned with standard RCA recipes, followed by a thermal oxidation process to form 4.5-nm-thick dry SiO<sub>2</sub> layer as a tunnel oxide in an atmospheric pressure chemical vapor deposition (APCVD) furnace. Right after the growth of tunnel oxide, poly-Si<sub>0.8</sub>Ge<sub>0.2</sub> was formed on the oxide immediately by low pressure chemical vapor deposition. The deposition of Si<sub>0.8</sub>Ge<sub>0.2</sub> was kept at 550 °C and the pressure was controlled to be 460

<sup>a)</sup>Electronic mail: tcchang@mail.phys.nsysu.edu.tw

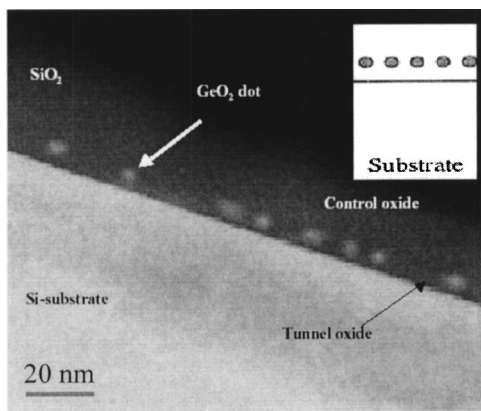


FIG. 1. The cross-sectional TEM micrograph of an oxide/GeO<sub>2</sub> nano-dots/oxide stacked structure.

mTorr. The flow rate of the reaction gas of SiH<sub>4</sub> and GeH<sub>4</sub> was 60 and 8 sccm, respectively, and the Ge fraction was analyzed to be around 0.2 by Auger electron spectroscopy. Subsequently, the Si<sub>0.8</sub>Ge<sub>0.2</sub> layer was oxidized in an APCVD reactor at 950 °C and the Ge atoms would be segregated downward until they reach the tunnel oxide surface.<sup>9–11</sup> The Ge dots grew based on the Ostwald ripening mechanism,<sup>12</sup> in which the larger dots grew at the expense of the smaller dots. After the Si elements of the Si<sub>1-x</sub>Ge<sub>x</sub> layer are completely oxidized, the Ge nanocrystals tend to be oxidized into GeO<sub>2</sub> nano-dots as the oxidation process is not ceased. From the analysis of transmission electron microscopy (TEM), the control oxide capped on the GeO<sub>2</sub> nano-dots was estimated to be about 40 nm and the GeO<sub>2</sub> nano-dots were confirmed via x-ray absorption near-edge structure (XANES). Finally, the Al electrode was patterned and sintered. Electrical measurements were performed on the metal-insulator-semiconductor structures with GeO<sub>2</sub> nano-dots embedded between tunnel and control oxide.

A cross-sectional TEM micrograph of an oxide/GeO<sub>2</sub> nano-dots/oxide stacked structure is shown in Fig. 1. It is clearly observed the GeO<sub>2</sub> nano-dots are embedded between the tunnel oxide and control oxide, oxidized from the Si<sub>1-x</sub>Ge<sub>x</sub> layer, and are separated from each other. The inset schematically shows the gate stack arrangement in this study. The mean size and aerial density of the dots are estimated to be about 5.5 nm and  $4.3 \times 10^{11} \text{ cm}^{-2}$ , respectively, by TEM.

To confirm the existence of the composition of the GeO<sub>2</sub> nano-dots, x-ray absorption near-edge structure (XANES) is performed.<sup>13–15</sup> In XANES, a core electron is excited to higher bound or quasibound states, which contain information about coordination geometry and electronic aspects of the absorbing atom. Among most of the XANES studies, the standard materials with known valence are utilized as references, and compared with the unknown samples. Therefore, the measurements are frequently qualitatively analyzed, not quantitatively. In this work, we used Ge powder, GeO<sub>2</sub> powder, and Si<sub>0.8</sub>Ge<sub>0.2</sub> epitaxial layer on Si as the standard materials and our investigated sample with nano-dots observed as the unknown sample. The x-ray source is extracted from the National Synchrotron Radiation Research Center. As shown in Fig. 2, the shift of absorption edge (roughly the center of the intensity jump) is an index of the Ge oxidation state. The obvious edge shift from the Ge edge and the high

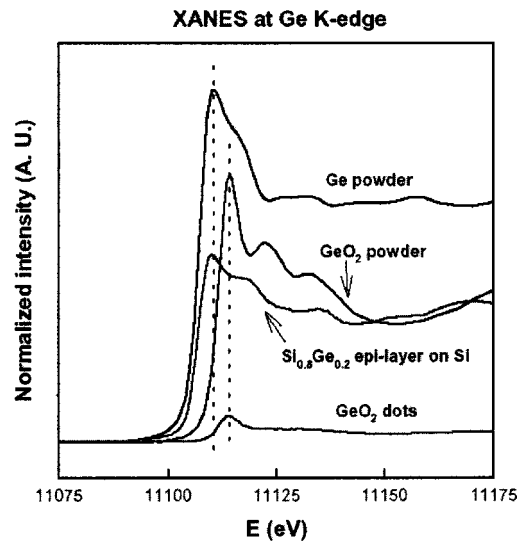


FIG. 2. The XANES spectra of the investigated sample and standard samples.

degree of similarity between the XANES results of the sample with nano-dots and GeO<sub>2</sub> standard reveal that Ge is oxidized. Its oxidation state is very close to GeO<sub>2</sub>.

Figure 3 shows the capacitance–voltage (*C*–*V*) hysteresis after the bidirectional bias sweeps between 5 V and (–5) V. It is found that a low operating voltage, 5 V, causes a significant threshold-voltage shift up to ~0.45 V, which is sufficient to be defined as “1” or “0” for the logic-circuit design. It is worth noting that the hysteresis is counterclockwise, which is due to substrate injection from the electrons of the deep inversion layer and holes of the deep accumulation layer of the Si substrate.<sup>16</sup>

Figure 4 demonstrates the band diagrams of the operation of the distributed charge storage with GeO<sub>2</sub> nano-dots. The “write” and “erase” operation with different gate polarities of the memory device are exhibited. When the device is written or programmed, the electrons directly tunnel from the Si substrate through the tunnel oxide, and are trapped in the GeO<sub>2</sub> nano-dots. When the device is erased, the electrons may tunnel back to the deep accumulation layer of Si substrate. The control oxide is utilized to prevent the

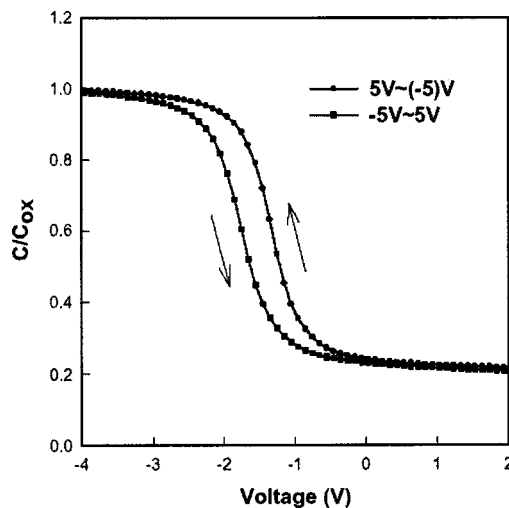


FIG. 3. The capacitance–voltage hysteresis after the bidirectional bias sweeps between 5 and (–5) V.

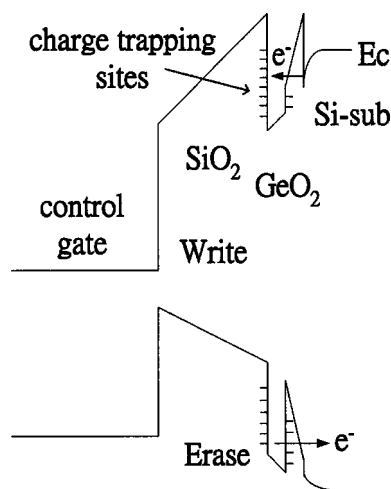


FIG. 4. The band diagrams of the operation of the distributed charge storage with  $\text{GeO}_2$  nano-dots.

carriers of gate electrode from injecting into the  $\text{GeO}_2$  nano-dots by Fowler–Nordheim tunneling. It is believed that during the oxidation process of the Ge nanocrystals into  $\text{GeO}_2$  nano-dots, there are defects or traps created in the interfaces between  $\text{GeO}_2$  dots and tunnel and control oxide. When the device is under programming, the injected electrons will be captured in the interfacial traps of the  $\text{GeO}_2$  dots and contribute to a threshold voltage shift (memory window). It is concerned about whether the storage of  $\text{GeO}_2$  nano-dots is as reliable as other insulating thin films. The reliability issues such as endurance and retention of the memory device should be taken into account and are currently under investigation.

In summary, a distributed charge storage with  $\text{GeO}_2$  nano-dots is shown. The mean size and aerial density of the dots are estimated to be about 5.5 nm and  $4.3 \times 10^{11} \text{ cm}^{-2}$ , respectively. The composition of the  $\text{GeO}_2$  dots is confirmed

by the XANES measurements. In electrical analyses, a significant memory effect is observed with a threshold voltage shift of 0.45 V under 5 V operation. Also, a physical model is proposed to explain the charge storage via the interfacial traps of  $\text{GeO}_2$  nano-dots. Further works about the research on the reliability issues are currently under investigation.

This work was performed at National Nano Device Laboratory and the National Synchrotron Radiation Research Center and was supported by National Nano Device Laboratory under Contract No. 92A0500001 and the National Science Council of the Republic of China under Contract Nos. NSC92-2112-M-110-020 and NSC92-2215-E-110-006.

<sup>1</sup>D. Kahng and S. M. Sze, *Bell Syst. Tech. J.* **46**, 1288 (1967).

<sup>2</sup>J. D. Blauwe, *IEEE Trans. Nanotechnology* **1**, 72 (2002).

<sup>3</sup>M. H. White, Y. Yang, A. Purwar, and M. L. French, *IEEE International Nonvolatile Memory Technology Conference*, 1996, p. 52.

<sup>4</sup>M. H. White, D. A. Adams, and J. Bu, *IEEE Circuits Devices Mag.* **2000**, 22.

<sup>5</sup>H. E. Maes, J. Witters, and G. Groeseneken, *Proceedings of the 17 European Solid State Devices Research Conference Bologna 1987*, p. 157.

<sup>6</sup>S. Tiwari, F. Rana, K. Chan, H. Hanafi, C. Wei, and D. Buchanan, *Tech. Dig. - Int. Electron Devices Meet.* **1995**, 521.

<sup>7</sup>J. J. Welsler, S. Tiwari, S. Rishton, K. Y. Lee, and Y. Lee, *IEEE Electron Device Lett.* **18**, 278 (1997).

<sup>8</sup>Y. C. King, T. J. King, and C. Hu, *Tech. Dig. - Int. Electron Devices Meet.* **1998**, 115.

<sup>9</sup>J. Rappich, I. Sieber, and R. Knippelmeyer, *Electrochem. Solid-State Lett.* **4**, B11 (2001).

<sup>10</sup>F. K. LeGoues, R. Rosenberg, T. Nguyen, F. Himpsel, and B. S. Meyerson, *J. Appl. Phys.* **65**, 1724 (1989).

<sup>11</sup>J. Eugene, F. K. LeGoues, V. P. Kesan, S. S. Iyer, and F. M. d'Heurle, *Appl. Phys. Lett.* **59**, 78 (1991).

<sup>12</sup>W. Ostwald, *Z. Phys. Chem. (Leipzig)* **34**, 495 (1900).

<sup>13</sup>P. Zhang and T. K. Sham, *Appl. Phys. Lett.* **81**, 736 (2002).

<sup>14</sup>S. Y. Ha, J. Park, T. Ohta, G. Kwag, and S. Kim, *Electrochem. Solid-State Lett.* **2**, 461 (1999).

<sup>15</sup>G. Dalba, P. Fornasini, R. Grisenti, F. Rocca, and I. Chambouleyron, *Appl. Phys. Lett.* **81**, 625 (2002).

<sup>16</sup>D. N. Kouvatso, V. L. Sougleridis, and A. G. Nassiopoulou, *Appl. Phys. Lett.* **82**, 397 (2003).